DOI: 10.24996/ijs.2026.67.4.31

ISSN: 0067-2904

Spectroscopic Study of the Influence of Corona Discharge Polarity on Air Discharge Characteristics in Liquid Electrodes System

Lubna Salah Ahmed *, Qusay Adnan. Abbas
University of Baghdad, College of Science, Department of Physics

Received: 26/ 6/2024 Accepted: 12/ 5/2025 Published: 30/ 4/2026

Abstract:
In this work, the influence of positive and negative corona discharges on the variation of air gap discharge characteristics with applied voltage under atmospheric pressure in the tap water electrodes system has been investigated. The discharge characteristics included emission spectra, electron temperature, electron number density, Debye length and plasma frequency. The results show no effect of polarity of space charge on the emission peaks. While the intensity of emission peaks increases when the presence of the negative space charge forms the negative corona discharge. Increasing the applied voltage increases the (T_e , n_e , ω_{pe}) plasma parameters while parameters (λ_D , N_D) decrease. The types of corona discharge do not affect the behavior of plasma parameters with the increased applied voltage, but it changes in value either rising or falling. The behavior of the discharge characteristics at the applied voltage range 0-25 kV showed different behavior when the applied voltage was greater than 25 kV in both types of corona discharge with a greater rate when the positive corona discharge was established.

Keywords: Corona discharge, Liquid electrode, Electron temperature, electron number density, spectroscopic emission, tap water.

دراسة طيفية لتأثير قطبية تفريغ كورونا على خصائص تفريغ الهواء في نظام الاقطاب السائلة

لبنى صلاح احمد* , قصي عدنان عباس
قسم الفيزياء ,كلية العلوم ,جامعة بغداد

الخلاصه
في هذا العمل، تم دراسة تأثير تفريغ كورونا الموجب والسالب على تغاير خصائص التفريغ الكهربائي الفجوة الهوائية مع الجهد المسلط عند الضغط الجوي لنظام الاقطاب السائلة. حيث شملت خصائص التفريغ أطياف الانبعاث ودرجة حرارة الإلكترون وكثافة عددية الإلكترونات وطول ديباي وتردد البلازما. فقد أظهرت النتائج عدم وجود تأثير لقطبية الشحنة الفضائية على قمم الانبعاث. بينما تزداد شدة قمم الانبعاث عند وجود الشحنة الفضائية السالبة التي شكلت تفريغ كورونا السالب. تؤدي زيادة الجهد المطبق إلى زيادة معلمات البلازما (T_e ,n_e , ω_{pe}) بينما تنخفض المعلمات (λ_D ، N_D) لا تؤثر أنواع تفريغ الهالة على سلوك معلمات البلازما لكنها تتغير في القيمة مع زيادة الجهد المطبق كذلك أظهر سلوك خصائص التفريغ عند نطاق الجهد المسلط 0–25 كيلو فولت سلوكًا مختلفًا عندما يكون الجهد المسلط أكبر من 25 كيلو فولت في كلا النوعين من تفريغ كورونا بمعدل أكبر عند إنشاء تفريغ كورونا الموجب.

*Email: Lubna.s@Sc.Uobaghdad.edu.iq

1. Introduction

A corona discharge is a glow discharge that originates in a small region of high electric field intensity that encircles a sharply curved conductor at atmospheric pressure. This discharge has been the subject of extensive research, both independently and as a means of examining the mechanisms present in uniform field discharges. [1]. The corona discharge differs from a uniform field discharge in that one (or both) electrodes have a large curvature and breakdown first occurs in the high field strength region around this electrode. The electric field in the remaining gap is significantly lower, preventing the spark from completely breaking through.[1].

Corona discharge is classified into two types: positive and negative. The positive corona occurs when the curved or sharp electrode is connected to the positive terminal of the power source, and the negative corona occurs when the curved or sharp electrode is connected to the negative terminal. [2,3].

The corona discharge has many scientific and technological applications, such as in industry and medicine [4]. Ozone generation is an important application of corona discharge. The oxidative properties of this gas have been used for water treatment and odor control [5,6]. Corona discharge technology has been explored for a wide range of applications, including electro-spraying [7,8], semiconductor technology [9], airflow control [10], chemical compound decolorating [11], and food and water decontamination [12-14]. In the medical field, researchers have investigated its use in treating dental cavities through plasma generated by corona discharge [15] and in removing biofilms from tooth surfaces by exposing them to positive streamers or negative Trichel pulses [16].

This work presents the design and fabrication of a tap water treatment system, which includes electrodes, a power supply, and a treatment chamber. The influence of corona discharge polarity and high voltage between the liquid electrode and the water surface on plasma parameters and water characteristics will be studied in more detail.

2. Theoretical Calculation of Plasma Characteristics

To characterize the effect of corona discharge types on the gas discharge parameters, an optical emission spectroscope was used to determine the corona discharge parameters such as electron temperature (T_e), electron number density (n_e), Debye length (λ_D), and plasma frequency (W_{pe}).

2.1 Electron Temperature

The electron temperature (T_e) is an important parameter when describing the plasma state. Many methods can be used to determine the electron temperature. The Boltzmann plot method represents the most important method to estimate the electron temperature. To use the Boltzmann plot method, the local thermodynamic equilibrium must be applied, which is displayed as [17-18]:

$$\ln\left(\lambda_{mn} I_{mn}/g_m A_{mn}\right) = -E_m/kT_e + \ln\left(N/U\right) \quad (1)$$

where I_{mn}, λ_{mn}, and A_{mn} are the intensity, wavelength, and transition probability, respectively, corresponding to transition from m to n, g_m is a statistical weight, k is the Boltzmann constant, N is the number density of emitting species, and U is a partition function.

The electron temperature was calculated from the slope of the graph of $\ln\left(\lambda_{mn} I_{mn}/g_m A_{mn}\right)$ versus the energy E_m (eV). The slope of the straight line is equal to $(-1/kT_e)$.

2.2 Electron Number Density

The electron number density (n_e) was calculated using the Stark broadening impact, which is expressed as [17-19]:

$$n_e(cm^{-3}) = [\Delta\lambda/2\omega_s]N_r \quad (2)$$

Here $\Delta\lambda$ is the line's full width at half maximum (FWHM), and ω_s is the theoretical line full-width Stark broadening parameter equal to 10^{16} cm^{-3} for neutral atoms and 10^{17} cm^{-3} for single charged ions.

2.3 Debye Length

Debye length (λ_D) is a measure of the shielding distance or thickness of the sheath; it can be determined using the following formula [17-20]:

$$\lambda_D = \sqrt{\frac{\varepsilon_0 k T_e}{e^2 n_e}} \cong 69\sqrt{\frac{T_e(K^\circ)}{n_e(m^{-3})}} \cong 743\sqrt{\frac{T_e(eV)}{n_e(cm^{-3})}} \quad (3)$$

here ε_0 is the permittivity of free space, k is the Boltzmann constant, and e is the electronic charge.

2.4 Plasma Frequency

Plasma frequency is an important plasma characteristic that differentiates plasma frequencies for electrons. This parameter represents the characteristic frequency of electrostatic oscillation caused by the close proximity of charges for electrons (e) in the plasma due to their small distance. The plasma frequency is determined by [17-20]:

$$\omega_{pe} = \sqrt{\frac{n_e e^2}{m_e \varepsilon_o}} \quad \text{(rad/sec)} \quad (4)$$

Where m_e is the electron mass.

2.5 The Plasma Parameter (N_D)

The plasma parameter (N_D) describes the number of charged particles in the Debye sphere and can be calculated using the formula [21]:

$$N_D = n\frac{4}{3}\pi\lambda_D^3 = 1.38 \times 10^6 T^{3/2}/n^{1/2} \quad (T \text{ in } ^\circ K) \quad (5)$$

where Te is the electron temperature (in K), and n is the plasma number density (in cm^{-3}). According to the above equation, N_D must be much greater than unity to achieve the collective characteristic of plasma: $N_D >> 1$ [17].

3. Experimental part

Figure (1) shows the schematic diagram of the system used in this work. The setup included a high-voltage DC power source with a maximum high voltage of 45 kV and a cylindrical glass vessel with a volume of 500 cm^3, filled with 100 cm^3 tap water, which is used as the liquid electrode (representing the active electrode). A 0.07 mm diameter capillary tube was used to seal the end of the glass vessel close to the water's surface where the water drop was formed at the capillary tube's end. The other electrode was a circular disc with a diameter of 4 cm immersed inside the liquid tap water. The air gap between the liquid electrode and water surface was 1 cm, where the corona discharge was produced by applying a high voltage between the water's surface and the liquid electrode. The corona discharge image was captured by an iPhone 15 pro max camera with a resolution of 48 MP. Both types of corona discharge characteristics were detected by an optical emission spectrometer (model Thorlabs, made in Germany) by diagnosing the discharge emission light at a wavelength range of 320-740nm.

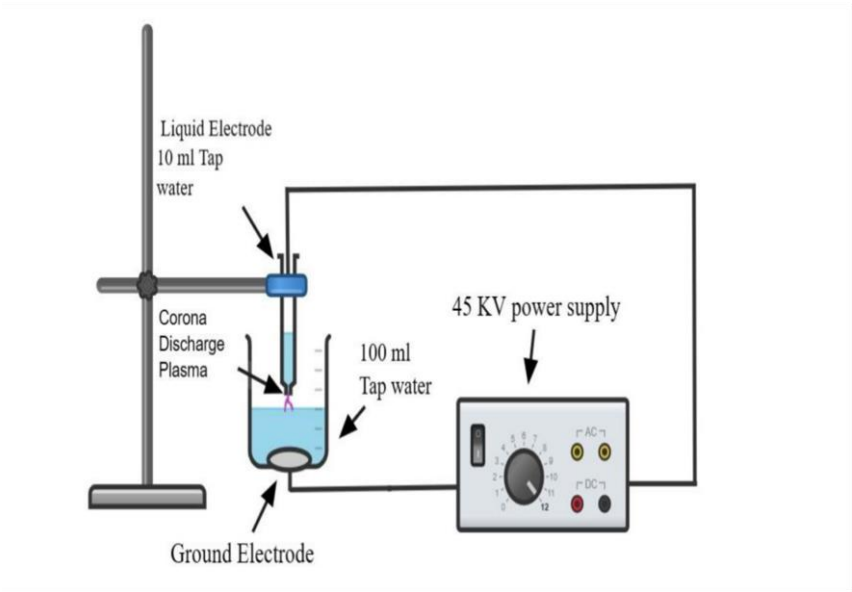

Figure 1: Schematic diagram of the liquid electrodes system.

4. Results and Discussion

4.1 Influence of Potential Difference on the Corona Discharge in Air Gap

The negative corona discharge formed at the tip of the capillary tube in the air gap above the water surface at atmospheric pressure is shown in the photograph in Figure (2). It can be observed that the water drop formed at the end of the capillary tube expands into a cone shape. The intensity of the negative corona discharge increased, and the cone size decreased with the increase in the applied voltage. As the applied voltage increased, the ionization region appeared very close to the active electrode and extended to the water surface. The increase in the applied voltage led to an increase in the number of corona branches near the active liquid electrode.

In addition, the effect of applying high voltage on the positive corona discharge at atmospheric pressure is also observed in Figure (3). This image also examines the increase in the intensity of the positive corona discharge near the active water electrode at the end of the capillary. In addition, as the applied voltage increased, the corona discharge was divided into many branches.

In summary, comparing Figures (2) and (3), it can be seen that the intensity of the negative corona discharge was higher than that of the positive corona discharge. This behavior can be due to the increase of the high negative applied voltage causing a sharp increase of the electric field of the drift region of the negative corona discharge (i.e. increasing the electron/negative ion ratio) comparable with positive corona discharge. This result agrees with that of Goldman et al. [3], and Abbas [13].

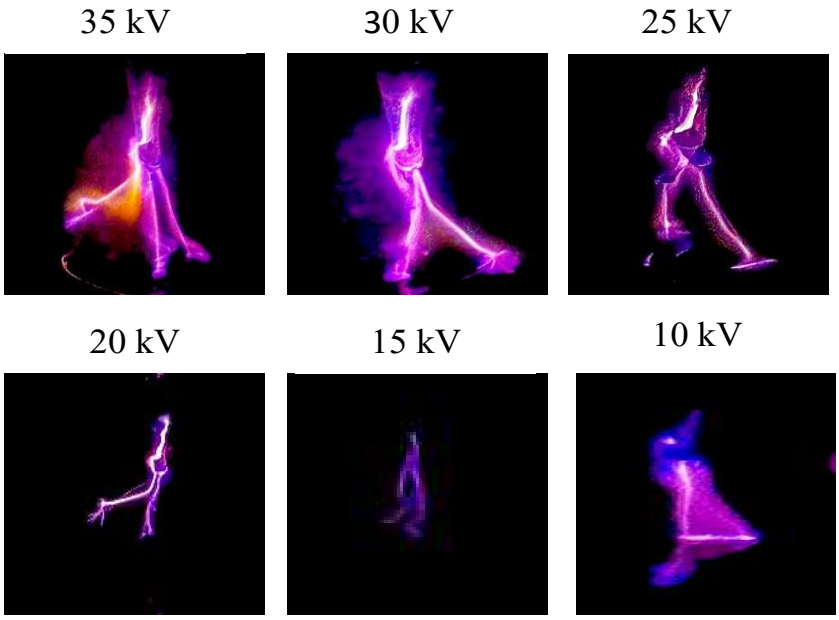

Figure 2: Influence of applied voltage on the negative corona discharge in the liquid electrodes system.

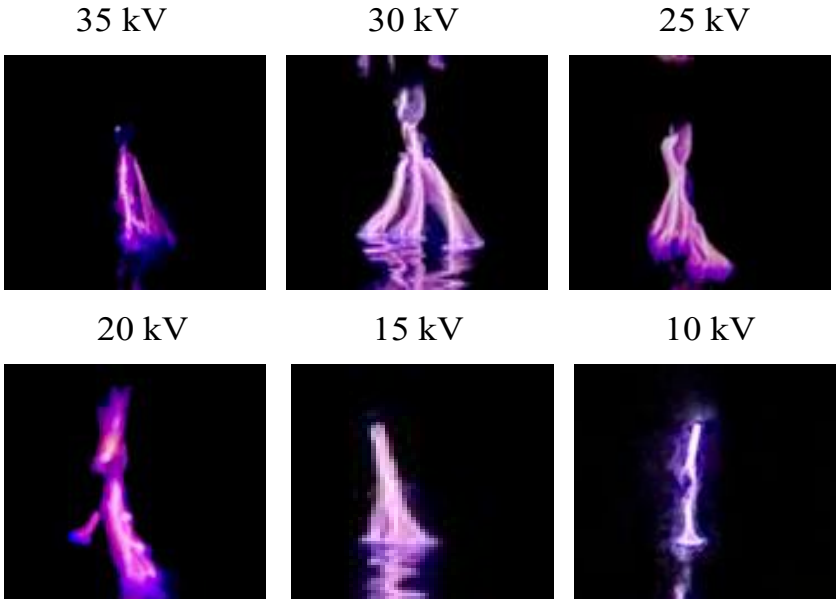

Figure 3: Influence of the applied voltage on the positive corona discharge in the liquid electrodes system.

4.2 Emission Spectra of Corona Discharge Plasma

Figures (4) detected the influence of positive applied voltage on the emission spectra of positive corona discharges in the wavelength range 320–740 nm under atmospheric air pressure in the tap water electrode system. The spectra illustrated one atomic emission peak of oxygen (O I), which appears at a wavelength of 405.48 nm, and seven ionic emission peaks of oxygen (O II) at wavelengths 353.65, 357.38, 374.95, 380.30, 399.28, 708.40, and 715.61nm. In addition, one neutral molecular emission peak of O_2 (O_2 I) also appeared at the wavelength of 373.01nm. As well as two emission peaks were also displayed in these spectra of the nitrogen element, one of them of atomic emission spectra (N I) that was located at wavelength 631.88 nm, and the other appeared to ionic emission spectra (N II) that was detected at a wavelength of 674.17 nm. It is clear from the spectra of this figure the fact that the increase of the positive applied voltage increased the ionization region from the active positive electrode

toward the water surface, which is due to the increase of the inelastic collisions between the positive space charge in the ionization region (positive space charge channels) with air species [22].

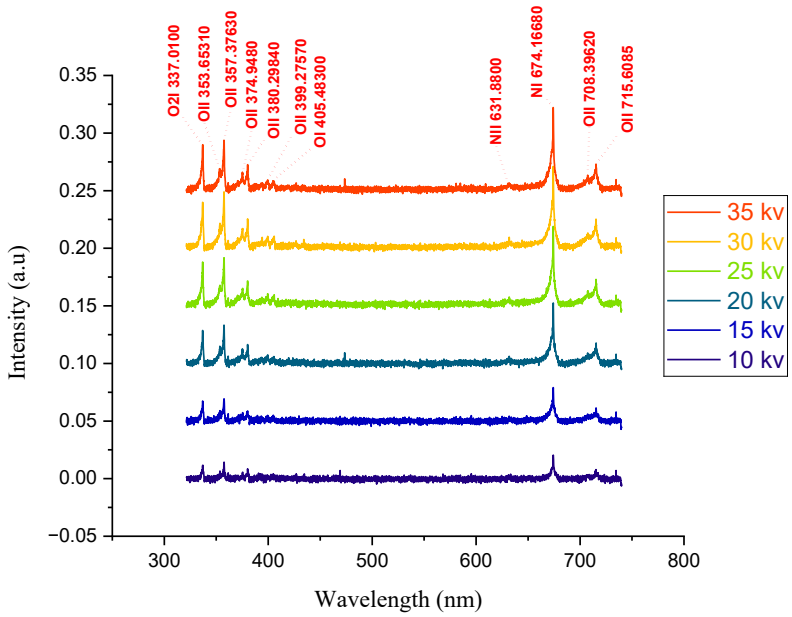

Figure 4: Optical emission spectra of the positive corona discharge as a function of the applied voltages under atmospheric air pressure.

Figure (5) investigated the influence of the negative applied voltage on the emission spectra of the negative corona discharge formed in the air gap at wavelength range 320-740 nm in a liquid electrode system. It is noticed from this figure that all emission peaks that appear in Figure (4) were also detected when the high negative voltages were applied to the active liquid electrode.

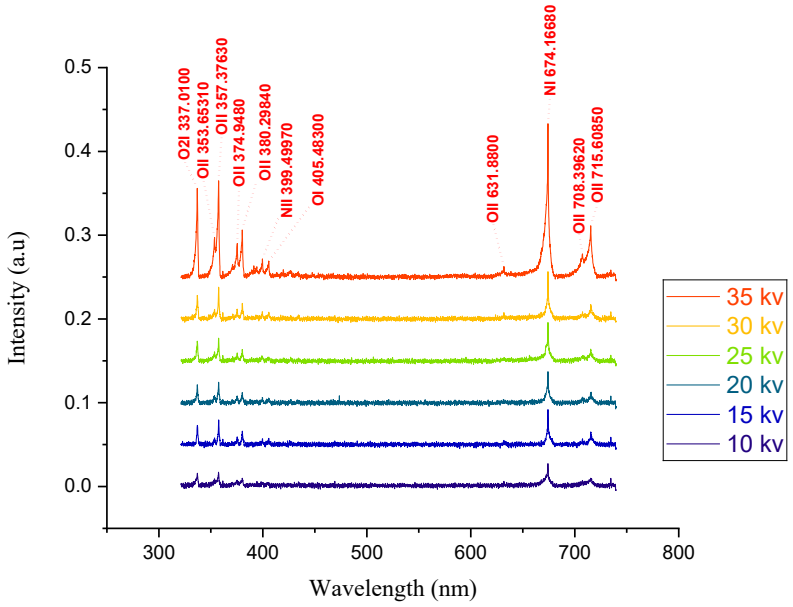

Figure 5: Optical emission spectra of the negative corona discharge as a function of the applied voltage under atmospheric air pressure.

The comparison of Figures (4) and (5) shows that the intensity of all emission peaks increased at an increased rate when the high negative voltage was applied to the active liquid electrode. This behavior makes sense because positive ions predominate in the positive corona, while negative ions are more prevalent in the negative corona due to differences in ionization mechanisms. The increase of the high negative applied voltage causes sharp increase of the electric field of the drift region of the negative corona discharge (i.e. increasing the electron/negative ion ratio) comparable with positive corona discharge [3].

4.3 Effect of the high applied voltage on the characteristics of both types of corona discharges

In this section, the influence of the high voltage applied to the active liquid electrode on the positive and negative corona discharges characteristics was investigated in more detail. The variation of electron temperature as a function of the high applied voltage of positive and negative corona discharges is displayed in Figure (6). It is clear that the electron temperature (T_e) of both corona discharges under study slightly increased with the increase of the active electrode voltage. This increase of T_e was due to the increase of the gain energy of the electrons from the high applied voltage on the active electrode. On the other hand, the data also detected higher rate of T_e value in the positive corona discharge comparable to the negative corona discharge. This behavior makes sense because positive ions predominate in the positive corona, while negative ions are more prevalent in the negative corona due to differences in ionization mechanisms. The increase of the high negative applied voltage causes a sharp increase of the electric field of the drift region of the negative corona discharge (i.e. increasing the electron/negative ion ratio) comparable with positive corona discharge [3].

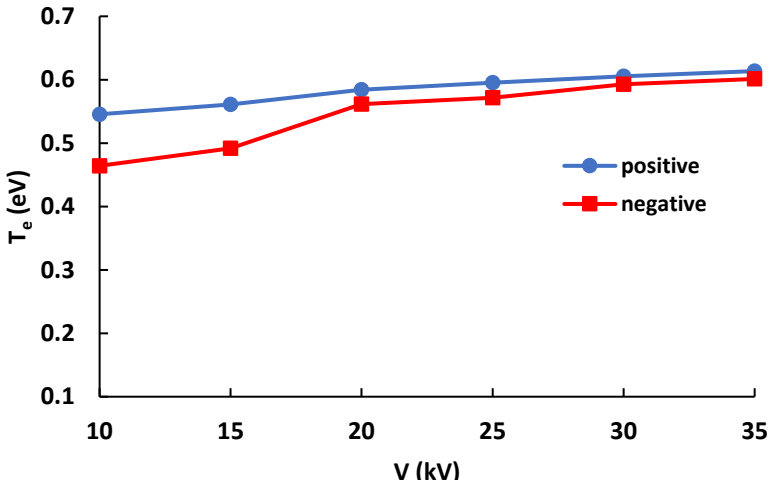

Figure 6: Electron temperature as a function of the applied voltage of the positive and the negative corona discharges**.**

Figure (7) shows the variation of the electron number density (n_e) with the applied voltages of positive and negative Corona discharges in the liquid electrode system. The data detected a non-linear increase of the electron number density with the applied voltage of both types of corona discharges. As the applied voltage increased from 0 kV to 25 kV, n_e increased slightly, and then it increased rapidly as the high applied voltage increased from 25 kV to 35 kV. The slight increase of ne when the applied voltage is smaller than 25 kV may be caused by the small energy gain of the electrons, which causes an increase of the electron attachment by the air species in both corona discharges. The applied voltage above 25 kV causes a further increase of the energy gained by the electron, reducing the electron attachment by the air species.

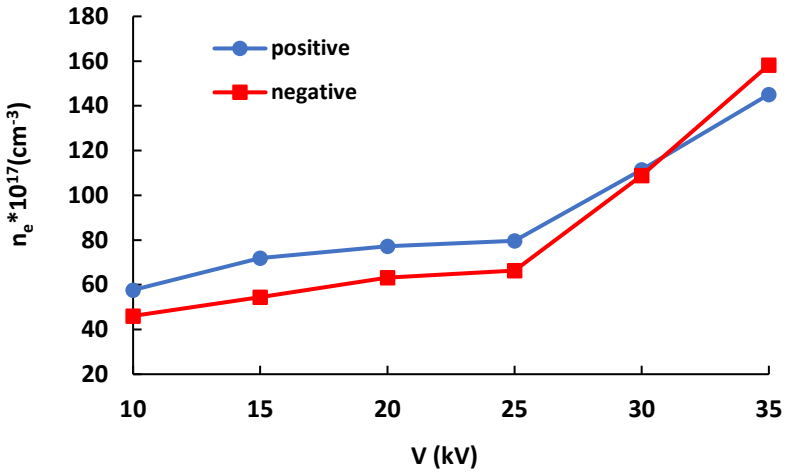

Figure 7: Electron number density as a function of the applied voltage of the positive and the negative corona discharges under atmospheric pressure.

Furthermore, Figure (8) depicts the variation of Debye length with the applied voltage of the two types of corona discharges under atmospheric pressure. In the 10-25 kV voltage range, the Debye length reduced slowly, and then it reduced sharply when the applied voltage increased from 25 kV to 35 kV. This behavior means that the effect of the space charge in both polarities became apparent in the applied voltage range of 25-35 kV.

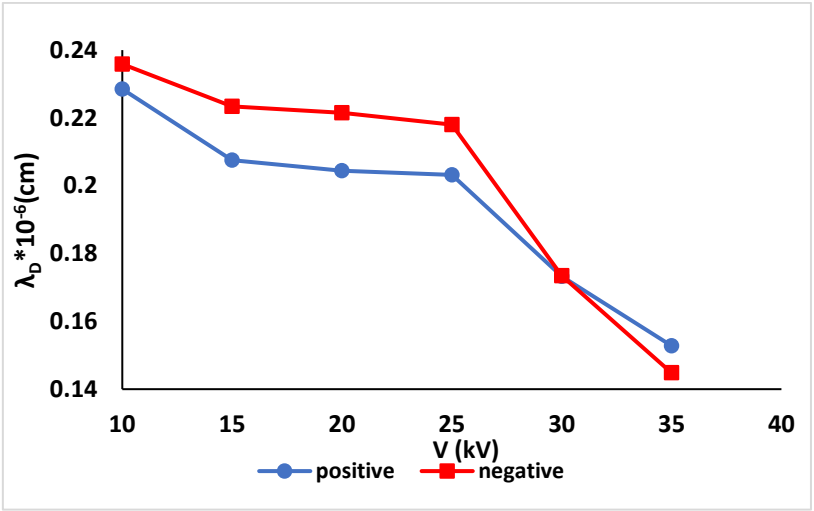

Figure 8: Debye length as a function of the applied voltage of positive and negative corona discharges at under atmospheric pressure.

Figure (9) shows the effect of the applied voltage on the plasma frequency of both corona discharges under study. The high plasma oscillation in the applied voltage range of 25 -35 kV is due to the huge impact of space charge in this voltage range in both types of corona discharges.

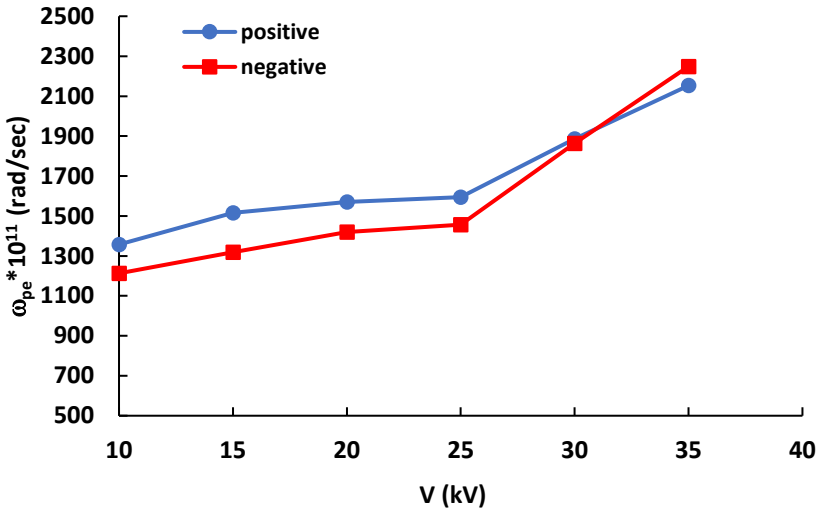

Figure 9: Plasma frequency versus applied voltage of positive and negative corona discharges under atmospheric pressure.

Finally, the variation of the plasma parameter (N_D) with the applied voltage of both kinds of corona discharges is illustrated in Figure (10). In the voltage range smaller than 25 kV, a slight variation of N_D was noticed with different behavior of space charge polarity, which depends on the corona discharge polarity. While at the voltage range of 25-35 kV, the space charge was suddenly reduced in both kinds of corona discharges.

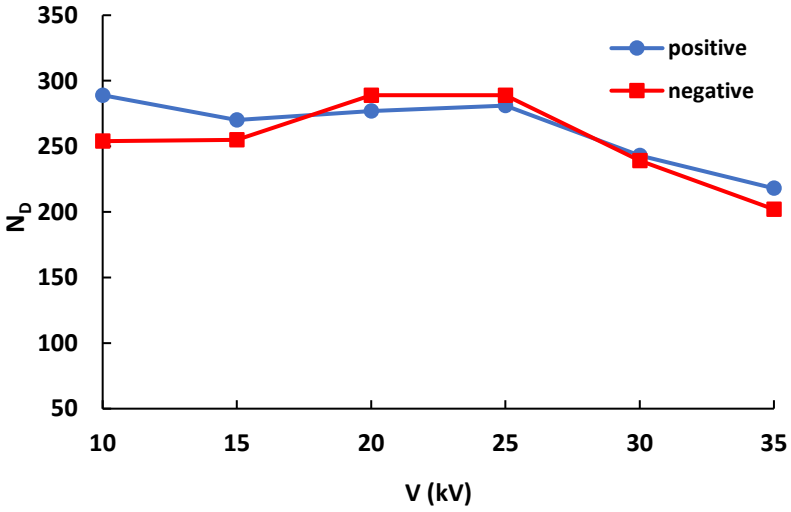

Figure 10: The variation of plasma parameter as a function of applied voltage of the positive and the negative Corona discharges at atmospheric pressure.

5. Conclusions

This work investigates the effects of positive and negative corona discharges on the characteristics of plasmas formed in an air gap between an active liquid electrode and a tap water surface under atmospheric pressure. The data showed that the corona discharge type at different voltages slightly affects the emission spectra of the corona discharge. However, the emission intensity of all emission peaks of the negative corona discharge is higher than that of the positive corona discharge. The effect of the applied voltage on plasma parameters (T_e , n_e , λ_D, ω_{pe} ,N_D) was studied. The parameters (T_e , n_e , ω_{pe}) increased, while parameters (λ_D , N_D) decreased with the increase of the applied voltage . However, it was observed that the type of

corona discharge did not affect the behavior of the plasma parameters with the applied voltage; it only changed their values, either rising or falling. The behavior of both corona discharges depends on the value of the applied voltage, leading to different behaviors when the applied voltage is higher than 25 kV.

References

[1] B. Maskell, "The effect of humidity on a corona discharge in air," 1970.

[2] M. K. Jassim, E. A. Jawad, and J. K. Alsaide, "Effect of Temperature on the Working Parameters of Negative Corona Discharge with Coaxial Electrodes Configuration," *Iraqi Journal of Science,* vol. 60, no. 9, pp. 1977-1984, 2019.

[3] M. Goldman, A. Goldman, and R. Sigmond, "The corona discharge, its properties and specific uses," *Pure and Applied Chemistry,* vol. 57, no. 9, pp. 1353-1362, 1985.

[4] P. Dordizadeh, K. Adamiak, and G. P. Castle, "Numerical investigation of the formation of Trichel pulses in a needle-plane geometry," *Journal of Physics D: Applied Physics,* vol. 48, no. 41, p. 415203, 2015.

[5] J. Chen and J. H. Davidson, "Ozone production in the positive DC corona discharge: Model and comparison to experiments," *Plasma chemistry and plasma processing,* vol. 22, pp. 495-522, 2002.

[6] J. Skalný, J. Országh, Š. Matejčík, and N. Mason, "Ozone generation in positive and negative corona discharge fed by humid oxygen and carbon dioxide," *Physica Scripta,* vol. 2008, no. T131, p. 014012, 2008.

[7] A. Jaworek, A. Sobczyk, T. Czech, and A. Krupa, "Corona discharge in electrospraying," *Journal of Electrostatics,* vol. 72, no. 2, pp. 166-178, 2014.

[8] H. Osman, G. P. Castle, and K. Adamiak, "Numerical study of particle deposition in electrostatic painting near a protrusion or indentation on a planar surface," *Journal of Electrostatics,* vol. 77, pp. 58-68, 2015.

[9] R. Thyen, A. Weber, and C.-P. Klages, "Plasma-enhanced chemical-vapour-deposition of thin films by corona discharge at atmospheric pressure," *Surface and Coatings Technology,* vol. 97, no. 1-3, pp. 426-434, 1997.

[10] E. Moreau, "Airflow control by non-thermal plasma actuators," *Journal of physics D: applied physics,* vol. 40, no. 3, p. 605, 2007.

[11] H. Wang, J. Li, and X. Quan, "Decoloration of azo dye by a multi-needle-to-plate high-voltage pulsed corona discharge system in water," *Journal of Electrostatics,* vol. 64, no. 6, pp. 416-421, 2006.

[12] M. A. Malik, A. Ghaffar, and S. A. Malik, "Water purification by electrical discharges," *Plasma sources science and technology,* vol. 10, no. 1, p. 82, 2001.

[13] Q. A. Abbas, "Effects of Positive Corona Discharge on PH Value of Tap and Distilled Waters in Liquid system," *Al-Nahrain Journal of Science,* vol. 16, no. 4, pp. 141-144, 2013.

[14] Q. A. Abbas, M. H. Dwech, F. Y. Hadi, and F. A. Mutlak, "Comparison the Formation of Spark Corona Discharge between Tap and distilled Waters at Liquid Electrode System," *Baghdad Science Journal,* vol. 10, no. 1, pp. 237-242, 2013.

[15] R. E. Sladek, E. Stoffels, R. Walraven, P. J. Tielbeek, and R. A. Koolhoven, "Plasma treatment of dental cavities: a feasibility study," *IEEE Transactions on plasma science,* vol. 32, no. 4, pp. 1540-1543, 2004.

[16] Z. Kovalova, M. Zahoran, A. Zahoranová, and Z. Machala, "Streptococci biofilm decontamination on teeth by low-temperature air plasma of dc corona discharges," *Journal of physics D: applied physics,* vol. 47, no. 22, p. 224014, 2014.

[17] F. F. Chen, Introduction to Plasma Physics and Controlled Fusion, vol. 1, New York: Plenum Press, 1984.

[18] Z. M. Abbas and Q. A. Abbas, "Characterization of Magnetized-Plasma System Induced by Laser," *Iraqi Journal of Physics,* vol. 21, no. 4, pp. 45-55, 2023.

[19] A. K. Bard and Q. A. Abbas, "Influence of cylindrical electrode configuration on plasma parameters in a sputtering system," *Iraqi journal of Science,* vol. 63, no. 8, pp. 3412-3423, 2022.

[20] Q. A. Abbas, A. F. Ahmed, and F. A.-H. Mutlak, "Spectroscopic analysis of magnetized hollow cathode discharge plasma characteristics," *Optik,* vol. 242, p. 167260, 2021.

[21] Z. M. Hasan and Q. A. Abbas, "Influence of AC Frequency on Hollow Magnetron Sputtering Discharge Parameters," *Iraqi Journal of Physics,* vol. 22, no. 1, pp. 31-41, 2024.
[22] A. Fridman and L. A. Kennedy, *Plasma physics and engineering*. CRC press, 2004.